DOI: 10.1002/ejic.201000107

Solid-State Structures and Properties of Europium and Samarium Hydrides

Holger Kohlmann*[a]

Keywords: Europium / Samarium / Hydrides / Neutron diffraction / X-ray diffraction

The structural chemistry of europium and samarium hydrides in the solid state is very rich, ranging from typical ionic hydrides following the hydride-fluoride analogy to complex transition metal hydrides and interstitial hydrides. While crystal structure, electrical, and magnetic properties suggest that europium is divalent in all hydrides investigated so far, samarium is easily transformed to a trivalent oxidation state in its hydrides and shows similarities to other lanthanide(III) hydrides. The problem of neutron absorption of europium and samarium, hampering crystal structure solution and limiting the available structural information, is discussed in detail, and practical solutions for neutron diffraction experiments are given.

1. Introduction

Metal hydrides are fascinating in inorganic chemistry because of their extremely versatile chemical bonding, crystal structures, and physical properties. Its medium electronegativity, small size and mass enable hydrogen to engage in ionic bonding with alkaline or alkaline earth metals, in covalent bonding to group 13 and 14 hydrides or as in homoleptic hydrido transition metal complexes, and finally also as an interstitial element in the metallic hydrides of some transition metals.[1] On the application side, metal hydrides have attracted a great deal of attention as hydrogen storage materials,[2] providing the means to safely store hydrogen, which might serve as an environmentally friendly and efficient energy carrier in the future.

For both basic and applied aspects, structural investigations have contributed considerably to the understanding of the factors governing chemical bonding, maximum hydrogen content, and physical properties of metal hydrides. Crystal structure determination, however, is hampered by the fact that these compounds rarely form single crystals, which means that diffraction experiments have to be done on powders. Moreover, in most cases, neutron diffraction is indispensable to locate hydrogen atoms with reasonable accuracy. Despite these complications, the crystal structures of many metal hydrides have been solved by a combination of X-ray and neutron powder diffraction.[3]

A further problem occurs for elements with extremely high absorption for neutrons, for example, europium and samarium. In fact, at the beginning of our investigations, no full crystal structure of europium or samarium hydrides was available in the literature to the best of our knowledge, probably because of these practical problems with neutron absorption. Our aim was to extend the vast knowledge on lanthanum and mischmetall hydrides, such as the classical hydrogen storage material $LaNi_5$,[2] to europium and samarium. Europium is of further interest, since, due to its special electron configuration, it is easily stabilized in a divalent oxidation state and may thus substitute alkaline earth elements, especially strontium, owing to their very similar ionic radii. This might create interesting new compounds as a result of the magnetic and spectroscopic phenomena associated with its presence in a solid-state structure, an aspect yet largely unexplored. In a first step we investigated the crystal structures and some physical properties of europium and samarium hydrides, which are reviewed in this paper.

[a] FR 8.1 Anorganische Festkörperchemie, Universität des Saarlandes,
Am Markt, Zeile 3, 66125 Saarbrücken, Germany
Fax: +49-681-302-70652
E-mail: h.kohlmann@mx.uni-saarland.de

Holger Kohlmann was born in Sobernheim (Germany) in 1967, and studied chemistry at the Justus-Liebig University Gießen (Vordiplom 1990) and at Saarland University (Diplom 1993). He received his Ph.D. in the group of Prof. Dr. H. P. Beck at Saarland University for research on the crystal chemistry of actinide chalcogenides in 1996. From 1997 to 2000, he was a postdoc in Prof. Dr. K. Yvon's group in Geneva (Switzerland) investigating metal hydrides, before joining Prof. Dr. M. F. Nicol at the University of Nevada, Las Vegas (USA) as a postdoc working on high-pressure techniques. In 2001 he held a visiting assistant professor position at the physics department of UNLV. After returning to Germany, he completed a Habilitation in Inorganic Chemistry in 2009, where he currently holds a lecturer position (Akad. Oberrat).

In the following, the problem of neutron absorption in general and for europium and samarium in particular shall be briefly surveyed and a practical solution for neutron powder diffraction will be discussed, before the crystal structures and some properties of samarium and europium hydrides are presented in detail. The discussion focuses on those hydrides with completely solved crystal structures, including hydrogen (deuterium) positions.

2. Synthesis and Structural Characterization

Europium and samarium hydrides are usually prepared by solid–gas reaction of metals or intermetallic compounds with hydrogen, for example,

$Eu + H_2 \rightarrow EuH_2$
$2\ SmMg_2 + 7\ H_2 \rightarrow 2\ SmMg_2H_7$

or of mixtures of metals and metal hydrides with hydrogen, for example,

$4\ EuH_2 + 2\ Ir + H_2 \rightarrow 2\ Eu_2IrH_5$

in high-pressure autoclaves at elevated temperatures. Alternatively, multinary hydrides may be synthesized by solid-state reaction of mixtures of the binary hydrides, for example,

$EuH_2 + LiH \rightarrow EuLiH_3$.

In some cases, such solid-state reactions of binary hydrides have been performed under high pressure in multianvil presses, for example,

$6\ EuH_2 + 7\ MgH_2 \rightarrow Eu_6Mg_7H_{26}$ at 3.5 GPa.

Detailed synthesis conditions are found in the original literature cited in sections 4 and 5. All europium and samarium hydrides investigated in this study are sensitive to air. Therefore, all handling operations were performed in argon-filled glove boxes.

No matter which preparation techniques are chosen, in general the products are metal hydrides as fine powders. Hence, the structural characterization is usually based on a combination of X-ray (synchrotron) and neutron powder diffraction. For europium- and samarium-containing compounds, the latter technique needs some extra attention; this will be discussed in the following section. For neutron diffraction, deuterides are often used because of their lower incoherent scattering relative to ^1H. Because this study focuses on structural investigations by neutron diffraction experiments, discussions often refer to deuterides. However, differences between hydrides and deuterides are very small with respect to crystal structures and properties of interest for this study. Thus, conclusions drawn from the deuterides can generally be transferred to hydrides. For possible isotope effects in hydrides vs. deuterides see ref.[4]

Crystal structure refinements on powder diffraction data with the Rietveld technique were performed by using the computer programs FullProf[5] and GSAS.[6]

3. Neutron Scattering and Absorption for Europium and Samarium

3.1. Neutron Scattering and Absorption Cross Sections

For the collision of a thermal neutron with a free nucleus, the total scattering cross section is given by the sum of the scattering and absorption cross sections,

$\sigma_t = \sigma_s + \sigma_a$

where the scattering cross section is

$\sigma_s = \int |f(\theta)|^2 d\Omega$

$f(\theta)$ being the scattering amplitude and $d\Omega$ an element of solid angle.[7] By using the free scattering length in its complex form,

$a = a' - ia''$
$\sigma_s = 4\pi|a|^2$
$\sigma_a = (4\pi/k)a''$

in a first approximation and neglecting corrective terms dependent on the wave vector **k**, too small to be of practical relevance for thermal neutrons. Furthermore, (n,γ) resonances are ignored, which play a role only in a handful of nuclides, such as ^{113}Cd and some rare earth metal isotopes.[7] In condensed matter, the bound scattering length is given by

$b = b' - ib'' = [(A + 1)/A]a$

where A is the ratio of nucleus/neutron mass. For a single strongly bound nucleus, the scattering and absorption cross sections are

$\sigma_s = 4\pi|b|^2$
$\sigma_a = (4\pi/k_0)b''$

where k_0 is the magnitude of the incident wave vector. By considering the effects of nuclear spin and for unpolarized neutrons, the above becomes

$\sigma_s = \sigma_c + \sigma_i = 4\pi|b_c|^2 + 4\pi|b_i|^2$
$= 4\pi <b>^2 + 4\pi(<b^2> - <b>^2)$
$\sigma_a = (4\pi/k_0)b''$

where σ_c is the bound coherent and σ_i is the bound incoherent cross section. Thus, the scattering cross section, σ_s, is independent of the neutron energy, except for those nuclides with a significant (n,γ) resonance.

Some important differences between neutron and X-ray diffraction arise from the energy dependencies of the above-mentioned cross sections and the difference between the interactions of neutrons and X-rays with matter. While the scattering cross section, σ_s, is independent of the neutron energy in most cases, it does vary between isotopes of the same element. This allows for making use of isotope effects, which will be of importance for treating heavily absorbing materials (vide infra). Furthermore, neutrons are scattered at the nuclei, which, in contrast to electron clouds scattering X-rays, can be considered point scatterers in a first approximation. Thus, the scattering cross section, σ_s, is largely independent of the scattering angle, such that much more information is contained in high-angle reflections of neutrons as

compared to X-ray patterns. Finally, light atoms often have scattering lengths comparable to heavier ones. For these reasons, neutron diffraction yields more information on light atoms, thermal displacement of atoms, rotational order of complex groups, while X-ray data in general yields more accurate lattice parameters and heavy atom positions. Therefore, X-ray and neutron diffraction complement each other and are both indispensable for the solution of the structures of metal hydrides.

The absorption cross section, σ_a, is inversely proportional to k_0 and thus to the neutron velocity v. This dependence of σ_a on v is known as the $1/v$ law of neutron absorption.[8] Absorption processes are (n,γ) reactions (radiative capture), (n,p) reactions, (n,α) reactions, and (n,f) reactions (fission), and thus

$$\sigma_a = \sigma_\gamma + \sigma_p + \sigma_\alpha + \sigma_f$$

There is a much larger spread in σ_a (0.00019 barn $< \sigma_a <$ 49700 barn) than in σ_s values (0.01838 barn $< \sigma_a <$ 35.9 barn[8]). However, absorption cross sections are of appreciable value only for few isotopes, for example, σ_f for some actinides, σ_α for ^{6}Li and ^{10}B, σ_p for ^{3}He, and σ_γ for ^{113}Cd and some rare earth isotopes. As a consequence, σ_a values are so small for the majority of isotopes that large samples can be used in neutron scattering. Only four elements (natural isotope mixtures) exhibit $\sigma_a > 1000$ barn for neutrons at a wavelength of 179.8 pm:[8] cadmium and the rare earth metals samarium, europium, and gadolinium (Figure 1). They are used as neutron shielding materials in nuclear reactor technology, cadmium as flexible metal sheets and the rare earths in form of the oxides dispersed in paint or concrete.[9]

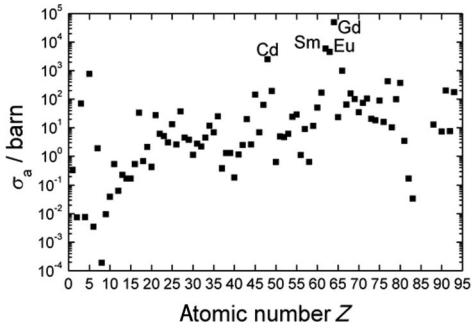

Figure 1. Neutron absorption cross sections, σ_a, of natural isotope mixtures of the elements at λ = 179.8 pm (thermal neutrons with velocity v = 2200 m/s; neutron energy E = 25.3 meV, corresponding to kT at room temperature) as a function of atomic number Z. Data taken from ref.[8] Please note the logarithmic scale on σ_a.

The neutron absorption of ^{nat}Sm is almost entirely determined by its ^{149}Sm (13.9% natural abundance) isotope. ^{nat}Sm shows a large resonance peak around 93 pm with almost 17000 barn (Figure 2).

The minimum in σ_a on the low-energy side around 200 pm is still at almost 6000 barn, that is, too high to be of practical interest to neutron powder diffraction. Only at wavelengths below 63 pm are absorption cross sections of less than 1000 barn reached (Figure 2), which makes it indispensable to use very short wavelengths for neutron powder diffraction studies of ^{nat}Sm-containing compounds.

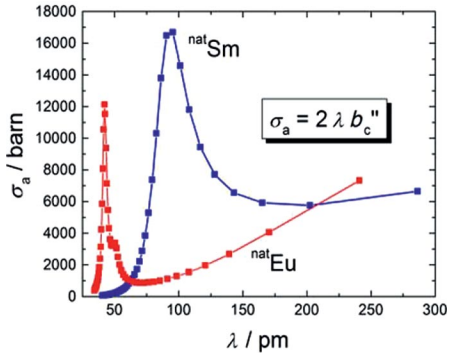

Figure 2. Neutron absorption cross section of the natural isotope mixtures of samarium, $\sigma_a(^{nat}Sm)$, and of europium, $\sigma_a(^{nat}Eu)$, as a function of neutron wavelength. Values calculated from the neutron wave vector **k** and the imaginary part of the scattering length a'' by $\sigma_a = (4\pi/k)a'' = (4\pi/k_0)b'' = 2\lambda b''$ (data for a'' taken from ref.[10]).

The neutron absorption of ^{nat}Eu is almost entirely determined by its ^{151}Eu isotope (47.8% natural abundance). ^{nat}Eu shows a large resonance peak at around 42 pm with over 12000 barn (Figure 2). Between this resonance effect and the low-energy region governed by the $1/v$ law, there is a minimum with 860 barn at 72.9 pm. This value is still appreciably high, but low enough to make neutron diffraction feasible.

3.2. Neutron Absorption of ^{nat}Sm and ^{nat}Eu – Practical Considerations

From the preceding discussion on neutron absorption cross sections, it follows that neutron powder diffraction on samarium- or europium-containing compounds may be feasible by using one of two approaches.

3.2.1. Use of Isotopically Pure Material

Since the extremely high absorption is mostly determined by one of the isotopes of samarium and europium, the use of another isotope can drastically reduce the absorption of the sample. However, this is an extremely costly strategy, which makes this method unsuitable for systematic studies on a larger number of different compounds, as for example in this work on the crystal chemistry of samarium and europium hydrides.

3.2.2. Using the Wavelength Dependence of the Absorption Cross Section of Natural Isotope Mixtures

As shown in Figure 2, σ_a values for ^{nat}Eu drop below 1000 barn at wavelengths below 37 pm and at a local minimum around 73 pm. For such σ_a values, the use of high-flux neutron diffractometers can overcome the still heavy absorption, unfortunately at the cost of resolution, which may be described as moderate at best (Figure 3). The best compromise for ^{nat}Eu-containing compounds seems to be

performing diffraction experiments at around λ = 73 pm with a high-flux neutron diffractometer such as D20[11] or D4[12] at the Institut Laue–Langevin (ILL, Grenoble, France). To reduce σ_a(^{nat}Sm) to a value below 1000 barn, one has to use wavelengths as short as 50 pm, leaving only D4 at the ILL as a suitable choice.

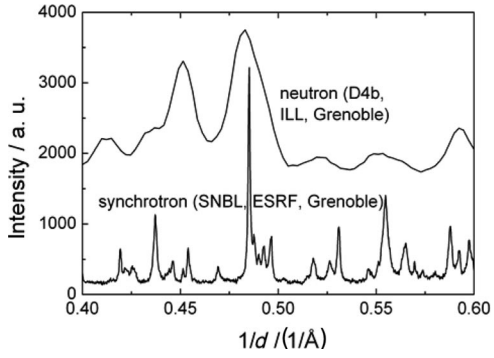

Figure 3. Parts of powder diffraction patterns of the same $Eu_6Mg_7D_{26}$ sample taken by using the high-resolution synchrotron diffractometer at BM1B [Swiss Norwegian Beamline at the European Synchrotron Radiation Facility (ESRF), Grenoble; λ = 60.054(1) pm; bottom] and the low-resolution neutron diffractometer D4b [ILL, Grenoble; λ = 70.647(8) pm; top], normalized to similar maximum intensities in arbitrary units. Abscissa d^* = $1/d$ = $2\sin\theta/\lambda$ = $Q/2\pi$ in 1/Å.

3.3. Transmission Factors for ^{nat}Eu- and ^{nat}Sm-Containing Compounds

The previous discussion has shown on a qualitative basis that neutron diffraction with samples containing natural isotope mixtures of elements such as Cd, Sm, Eu, or Gd seems to be feasible only under optimized experimental conditions. In order to prove this assumption, transmission factors will be calculated in this section for ^{nat}Eu-containing compounds. The highest europium concentration in deuterides is found in the binary compound EuD_2. Calculations will be performed for the optimum wavelength of 73 pm. For EuD_2 the linear absorption coefficient μ for λ = 73 pm is calculated by the equation

$$\mu = \Sigma_i N_i \sigma_{a,i} / V$$

where N_i is the number of atoms per unit cell of the absorbing element i, $\sigma_{a,i}$ is the neutron absorption cross section of the absorbing element i at the wavelength used, V is the unit cell volume, which yields a value of 2.067 mm^{-1}. This results in a small value of 0.48 mm for $1/\mu$, which is often used as a rule of thumb for an appropriate sample thickness for highly absorbing samples. From these data it is obvious that a standard neutron diffraction experiment, where cylindrical sample holders with diameters in the order of 10 mm are commonly used, will not give a high enough transmission even for the optimum wavelength. A drastic reduction in sample thickness is necessary; however, reduction of the cylinder diameter will also drastically reduce the amount of sample available for the experiment. Less costly in terms of sample volume is the use of double-walled cylinders, in which only the space between the inner and outer tubes will be filled with powder specimen. In this way, small sample thicknesses can be realized while still retaining appreciable sample volumes.

To illustrate this point, the transmission of EuD_2 has been calculated by using the program ABSOR[13] both for (a) a single-walled (4.5 mm diameter, 50% packing density) and (b) a double-walled cylinder [inner diameter of outer tube 9.15 mm, outer diameter of inner tube 7.96 mm, 50% packing density, resulting in the same sample volume as for case (a)]. Figure 4 clearly shows the drastic increase in transmission just by changing the sample geometry from cylindrical to annular (double-walled cylinder) while retaining the same sample volume. Moreover, another beneficial effect makes the use of double-walled cylinders favorable: Figure 4 also shows that the transmission for cylindrical samples exhibits a strong dependence on the diffraction angle, 2θ, while such dependence is almost negligible for the annular sample. This angle dependence is problematic in view of the crystal structure refinement by the Rietveld method. Because of the similarity of the angle dependence of the transmission [$I/I_0 = e^{-\mu d(2\theta)}$] and that of the temperature factor [$e^{-B(\sin\theta/\lambda)^2}$], uncorrected systematic errors of the former effect may be modeled by the Debye–Waller factor B in the above formula, which will refine to too low and even negative values if absorption is strong, that is, transmission is low. It has to be emphasized that this effect is not caused by the absorption as such, but by its dependence on the diffraction angle. For a neutron diffraction pattern collected on a EuD_2 sample with the geometry as given in Figure 2, refinements have been performed by using uncorrected patterns and patterns corrected for absorption effects. The only parameters showing significant changes are the Debye–Waller factors B, but they differ by less than 14% only, thus making the absorption correction almost obsolete.[14]

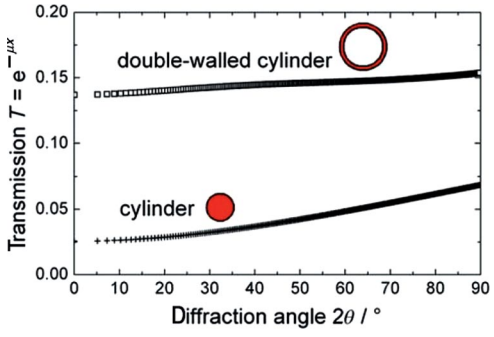

Figure 4. Transmission factors for identical volumes of EuD_2 (λ = 70 pm, linear absorption coefficient, μ = 2.067 mm^{-1}, 50% packing density) in a full cylinder (inner diameter 4.5 mm) and a double walled cylinder (annular sample with inner diameter of outer cylinder 9.15 mm, outer diameters of inner cylinder 7.96 mm, resulting in 0.6 mm annular thickness). Calculations were performed with the program ABSOR.[13]

A correct treatment of (n,γ) resonance effects also requires considering the imaginary part a'' of the coherent scattering length in the calculation of structure factors

F(*hkl*), which we could try after Bob Von Dreele has been kind enough to include wavelength-dependent *a''* data taken from ref.[10] in the computer program GSAS.[6] The effect on the structure refinements, however, is negligible.[14]

Even with the optimized geometry, the annular samples will have much smaller sample volumes as compared to those commonly used for standard nonabsorbing samples in single-walled cylinders (diameter ≈ 10 mm). Also taking into account that, even with the optimized wavelength, the neutron absorption is still very high, it is obvious that neutron powder diffraction on samples such as EuD_2 could only work with high-flux neutron diffractometers with efficient detectors such as D20[11] or the diffractometer D4[12] installed at the hot source (both ILL, Grenoble, France). Experiments on other diffractometers with higher resolution but lower neutron flux, such as D2b, did not yield useful data.

The neutron powder diffraction experiments on ^{nat}Eu and ^{nat}Sm hydrides described in detail in the following discussion, have in general confirmed the reasoning given above. Useful neutron powder diffraction data on ^{nat}Sm- and ^{nat}Eu-containing compounds could only be collected if *all* of the following conditions were fulfilled: (1) Use of a high-flux neutron diffractometer with efficient detectors; (2) careful choice of the wavelength; (3) optimized sample geometry with double-walled vanadium cylinders as sample holder (annular samples)

4. Solid-State Structures of Europium Hydrides

At the beginning of this study, no full crystal structure of any europium hydride was available in the literature to the best of our knowledge, probably because of severe problems with neutron absorption, as discussed above. Several europium hydrides had been investigated by X-ray diffraction, and the metal atom substructure had been determined; hydrogen (deuterium) positions, however, were not known. In the course of this study, some of these known europium hydrides have been fully structurally characterized and more ternary europium hydrides were discovered and characterized during systematic explorations of the systems Eu–Li–H, Eu–Mg–H, Eu–Pd–H, and Eu–Ir–H.

4.1. EuD_2 – A Test Case for Neutron Diffraction with ^{nat}Eu

As mentioned before, binary europium dihydride (deuteride) has got the highest neutron absorption of all known (investigated) europium hydrides, that is, it could be used as a test case for the strategy for neutron diffraction with ^{nat}Eu elaborated in the previous section. Europium dihydride attracted some interest in the past as a ferromagnetic semiconductor.[15] There have been claims for nonstoichiometric $EuH_{1.8–1.95}$,[16] thus raising questions about the presence of hydrogen defects and the valence state of europium. Its crystal structure, although proposed to belong to the orthorhombic $PbCl_2$ type structure,[15–17] could not be verified experimentally due to the above mentioned problems of locating hydrogen (deuterium) by neutron diffraction caused by the extremely high absorption of such samples. The aim of this study was thus to investigate the aspect of nonstoichiometry and locate hydrogen (deuterium) in europium dihydride (deuteride).

The neutron powder diffraction pattern indeed shows clearly discernible Bragg peaks with a high and sloped background due to the paramagnetic contribution of europium to neutron scattering (Figure 5). The crystal structure can be refined to good residual values, which results in atomic positional standard uncertainties on the fourth digit and uncertainties in interatomic distances of less than 0.2%.[14] Thus, structure refinement on europium hydrides by following the strategy outlined above yields meaningful crystal structure data, which are of almost comparable accuracy as those of other less absorbing samples. Crystal structure refinements have also been performed on data corrected for absorption effects by using the program ABSOR.[13] The only parameters showing significant changes with respect to the uncorrected data are the Debye–Waller factors *B*. They differ by less than 14%, however, thus making absorption correction unnecessary, unless accurate thermal displacement parameters are sought for.

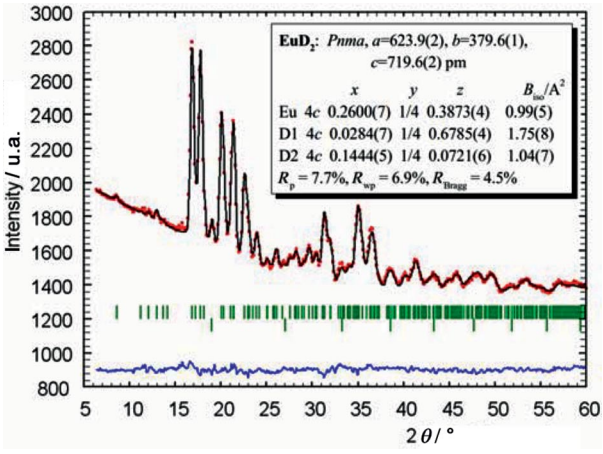

Figure 5. Observed (red circles), calculated (black solid line) and difference (bottom) neutron powder diffraction patterns of EuD_2 taken on D4 at the ILL, Grenoble (T = 293 K, λ = 70.5 pm). Bragg markers from EuD_2 (top) and vanadium from the sample holder (bottom).

Figure 6 shows a projection along the crystallographic *b* axis of the EuD_2 crystal structure. The $PbCl_2$-type arrangement shows trigonal EuD_6 prisms linked by common triangular faces along *b* to form columns. Further linking by common edges results in zigzag chains of interconnected prisms running along *a*. The complete coordination polyhedron around europium is a tricapped trigonal prism of deuterium atoms with nine Eu–D distances ranging from 238.3(5) to 275.9(3) pm (mean distances 255 pm). EuH_2 is thus isotypic to CaH_2,[18] SrH_2,[19] BaH_2,[20] and YbH_2.[21] The refined crystal structure is in accordance with a stoichiometric saltlike EuD_2 containing divalent europium. This contrasts reports in the literature on nonstoichiome-

try.[16] It is in agreement, however, with its semiconducting behavior,[16a] localized magnetic moments typical for Eu^{2+},[15b] volume increments,[22] and its classification as a member of the ionic branch of the $PbCl_2$-type family.[23]

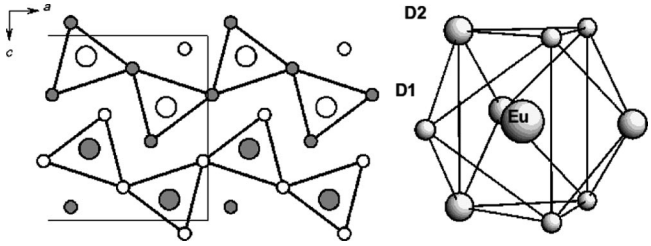

Figure 6. Crystal structure of EuD_2 ($PbCl_2$ type, space group type *Pnma*) in a projection along crystallographic *b* axis [Eu (large), D (small), *y* = 1/4 (empty symbols), *y* = 3/4 (filled symbols)] (left) and coordination polyhedron of europium in EuD_2 (right).

Thus, this structure determination could clarify questions about the stoichiometry and the valency of europium in EuD_2. More importantly, it has proven the feasibility of neutron powder diffraction on ^{nat}Eu-containing compounds by the method elaborated in the previous section.

4.2. Saltlike Ternary Europium Lithium and Europium Magnesium Hydrides

Ternary $EuLiH_3$ has been known for over 40 years, and an inverse cubic perovskite type structure has been proposed.[24] Hydrogen positions, however, could not be determined because of the above-mentioned problems with neutron diffraction. Our neutron powder diffraction data on $EuLiD_3$ taken with D4b (ILL, Grenoble, France) have proven this model to be correct. Europium [*d*(Eu–D) = 267.82(2) pm] and lithium [*d*(Li–D) = 189.38(2) pm] are cuboctahedrally and octahedrally surrounded by deuterium, respectively (Figure 7, right).[14] The crystal structure suggests that $EuLiH_3$ is a stoichiometric saltlike compound containing Eu^{2+}, which is in agreement with its red color, semiconducting properties, and Mössbauer spectroscopic investigations.[25]

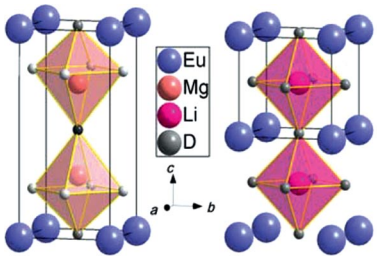

Figure 7. Crystal structures of $EuMg_2D_6$ (left, unitary structure type, D1 light gray, D2 middle gray, D3 dark gray) and of $EuLiD_3$ (right) in the cubic perovskite type (two unit cells of $EuLiD_3$ are shown).

While several ternary hydrides in the systems Ca–Mg–H, Sr–Mg–H, and Ba–Mg–H are known to exist, no europium magnesium hydrides were known at the beginning of this study.[26] The similarity of the ionic radii and chemical properties of strontium and europium suggested the possible existence of compounds analogous to $SrMgH_4$[27] and $Sr_2Mg_3H_{10}$.[28] Corresponding hydrogenation of intermetallic Eu–Mg compounds yielded the new compounds $EuMgH_4$ and $EuMg_2H_6$, where the latter surprisingly repre-

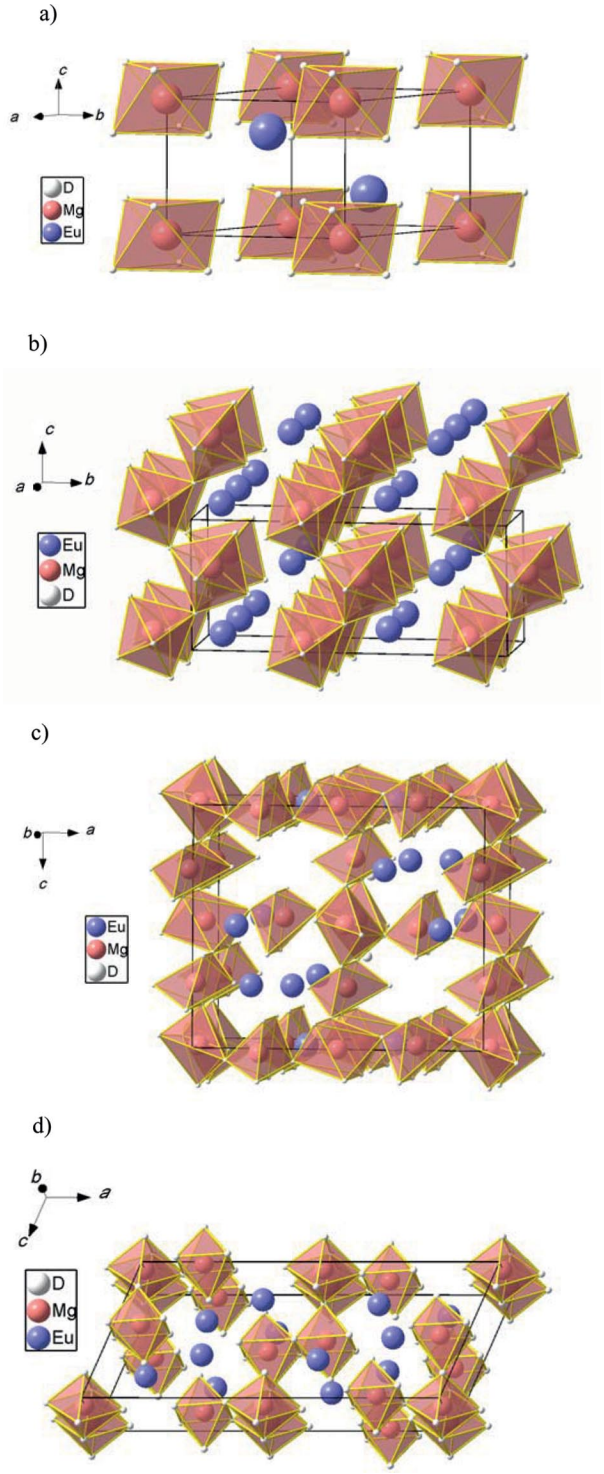

Figure 8. Crystal structures of europium magnesium deuterides with MgD_6 octahedra in (a) Eu_2MgD_6 (K_2GeF_6 type), (b) $EuMgD_4$ ($BaZnF_4$ type), (c) $Eu_6Mg_7D_{26}$ ($Ba_6Zn_7F_{26}$ type), (d) $Eu_2Mg_3D_{10}$ ($Ba_2Ni_3F_{10}$ type).

sents a stoichiometry not yet known in alkaline earth magnesium hydride chemistry.[29] Three more compounds, Eu_2MgH_6, $Eu_6Mg_7H_{26}$, and $Eu_2Mg_3H_{10}$, could be prepared at high pressures and high temperatures in a multianvil press and quenched to ambient conditions[30] (Figures 7 and 8). In addition to the absorption problem, structure determination for the latter three compounds was hampered by the fact that no single-phase samples could be prepared because of the special synthesis conditions. Furthermore, in the case of $Eu_6Mg_6H_{26}$, a very small monoclinic distortion of a pseudo-orthorhombic structure could only be detected by high-resolution synchrotron powder diffraction. This corresponds to a symmetry reduction from the orthorhombic $Ba_6Mg_7D_{26}$ to the monoclinic $Ba_6Zn_6F_{26}$-type structure (Figure 9), not seen in laboratory X-ray or neutron diffraction data. By fully implementing the complementary character of X-ray (synchrotron) and neutron diffraction, the structures of these three high-pressure phases were determined and refined simultaneously with use of two synchrotron [λ = 60.054(1) pm, Swiss/Norwegian Beamline BM1B, ESRF, Grenoble] and three neutron powder diffraction patterns [λ = 70.50(1) pm, D4b, ILL, Grenoble] with up to 182 free parameters.[30] The crystal structures of $EuMgD_4$ and $EuMg_2D_6$ were determined and refined from laboratory X-ray (Co-K_α radiation) and neutron diffraction data [λ = 80.45(1) pm, D20, ILL, Grenoble]. In the case of $EuMgD_4$, only neutron data could reveal the true symmetry, i.e. the distinction between the centrosymmetric $LaNiD_4$-type, in which also $BaMgD_4$ crystallizes, and the noncentrosymmetric $BaZnF_4$-type of the lighter homologue $SrMgD_4$ (Figure 9) could be made. The latter was proven to be the correct model, which makes sense because the smaller radii of Sr^{2+} and Eu^{2+} favor the smaller coordination number of nine in the structure with lower symmetry as compared to the higher coordination number thirteen of the larger Ba^{2+}.[29]

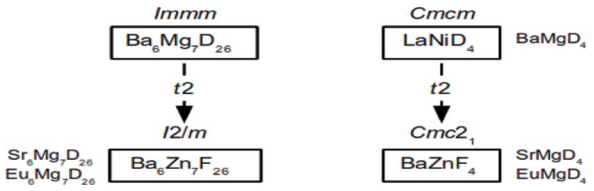

Figure 9. Bärnighausen symmetry tree with group subgroup relationships between europium and alkaline earth magnesium deuterides. Structure types inside boxes, further representatives outside boxes. Some structural data have been transformed crystallographically with respect to original literature data. Literature: $Ba_6Mg_7D_{26}$,[35] $Sr_6Mg_7D_{26}$,[36] $Eu_6Mg_7D_{26}$,[30] $BaMgD_4$,[37] $SrMgD_4$,[28] $EuMgD_4$.[29]

In analogy to ternary alkaline earth magnesium hydrides (deuterides),[31] all five europium magnesium hydrides (deuterides) exhibit MgD_6 octahedra as structural units. These octahedra are either isolated (Figure 8a, Eu_2MgD_6) or corner-sharing (Figures 8b and 7, $EuMgD_4$ and $EuMg_2D_6$).[29] Additional edge-sharing of MgD_6 octahedra, for example in $Eu_6Mg_7D_{26}$ and $Eu_2Mg_3D_{10}$ (Figures 8c and d), may be achieved by the use of high-pressure methods for the synthesis.[30] These phases, Eu_2MgH_6, $Eu_6Mg_7H_{26}$, and $Eu_2Mg_3H_{10}$, prepared under high pressure, show considerable volume contractions of 7.3%, 2.6%, and 3.1% with respect to the sum of the volumes of the binary hydrides.

The crystal structure of $EuMg_2D_6$ was determined and refined by a combination of X-ray and neutron powder diffraction data and can be described as a defect perovskite, in which every other layer of europium is missing according to the formula $Eu_{1/2}\square_{1/2}MgD_3 = EuMg_2D_6$. In order to rationalize this new crystal structure type, one may formally replace Li in the cubic perovskite $EuLiH_3$[14] by Mg while omitting half of the Eu^{2+} cations, thus keeping charges balanced. For a detailed description of the structural relationships, see the recent reviews.[32] Because of the missing Eu layers with respect to the perovskite, the MgD_6 octahedra become distorted, and the coordination number of one deuterium atom is reduced to two. The experimentally determined Mg–D distance (177 pm) is the shortest known in ionic magnesium hydrides, except for those prepared under high-pressure conditions. Only up to 60% of europium may be replaced by strontium under retention of the structure type,[33] in contrast to all other hydrides, where isotypic strontium compounds exist. No other compound adopting this structure type is known; however, $Na_5[MO_2][X]$ (M = Co, Ni, Cu; X = CO_3, S; for M = Cu also X = SO_4, SO_3) represents a substitutional variant of an antitype.[34] Sodium atoms correspond to those deuterium atoms in $EuMg_2D_6$ that are four- or sixfold coordinated, metal atoms M to the twofold coordinated deuterium positions. Oxygen atoms coordinated to metal atoms M sit on magnesium positions of the $EuMg_2D_6$ structure, the center of gravity, X, of the oxoanions on europium positions.

Except for $EuMg_2H_6$, all europium magnesium hydrides (Figure 8) are isotypic to fluorides. The crystal structures discussed above, interatomic distances, magnetic, and optical properties are consistent with ionic descriptions of europium magnesium hydrides containing Eu^{2+}, Mg^{2+} and H^-.

4.3. From Complex to Interstitial Hydrides – Ternary Europium Palladium and Europium Iridium Hydrides

Europium may replace alkaline earth metals, especially strontium, in ternary hydrides with transition metals as well. In contrast to the ternary hydrides with lithium or magnesium discussed before, these compounds show different chemical bonding behavior. This is not surprising, because the transition metals do not form ionic hydrides like lithium and magnesium, but interstitial-type hydrides. Therefore, the chemical bonding situation is expected to change with the ratio of europium to transition metal in the hydrides. This may be nicely illustrated on ternary europium palladium hydrides. The most europium-rich compound was found to be Eu_2PdH_4.[38] The crystal structure as determined on the deuteride shows PdD_4 tetrahedra having Pd–D distances consistent with covalent bonding (167

to 182 pm, Figure 10). A divalent oxidation state of europium can be inferred from magnetic susceptibility measurements, which are also in agreement with the crystal structure of the β-K_2SO_4 type.[38] Thus, the chemical bonding in this violet colored, semiconducting hydride may be described by an ionic limiting formula $(Eu^{2+})_2[PdH_4]^{4-}$, in which an 18-electron tetrahydridopalladate complex with covalent Pd–H bonding interacts electrostatically with Eu^{2+} cations in an ionic-type bonding. Theoretical calculations predict the band gap to be 0.23 eV.[39]

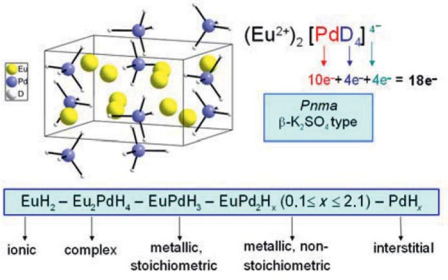

Figure 10. The crystal structure of Eu_2PdD_4 in the orthorhombic β-K_2SO_4-type structure, exhibiting complex 18-electron $[PdD_4]^{4-}$ complexes and chemical bonding in europium palladium hydrides with increasing palladium content from the left to the right.

The situation changes completely for hydrides richer in palladium. When EuPd is hydrogenated, its metal atom substructure changes from the CrB to the CsCl type, just opposite to the case of ZrCo.[38,40] Deuterium atoms were found to surround palladium in an octahedral fashion in the deuteride, yielding a cubic perovskite-type structure for $EuPdD_3$.[38] $EuPdH_3$ shows metallic properties and contains divalent europium.[41] The latter is in accordance with europium–deuterium distances from the crystal structure refinements, which also showed full occupancy of deuterium positions.[38] Thus, $EuPdH_3$ is a metallic hydride containing divalent europium with an ordered hydrogen (deuterium) distribution untypical for interstitial hydrides. Other cubic perovskite- and antiperovskite-type hydrides often show partial occupancy of hydrogen positions.[3b,42]

Typical interstitial hydrides are found when the cubic Laves phase, $EuPd_2$, which is richer in palladium, is hydrogenated. Metallic hydrides with variable hydrogen content $EuPd_2H_{0.1\le x\le 2.1}$ result, retaining the cubic Laves phase structure of the metal atom substructure.[38] Disordered hydrogen contributions are quite common in Laves phase hydrides,[43] some of which are used in anode materials of rechargeable Ni-MH batteries. Ternary europium palladium hydrides are a good example to show how bonding properties change from mainly ionic over mixed-ionic-covalent in complex hydrides to typical metallic interstitial hydrides.

Another peculiar aspect of the structural chemistry of complex hydrides is nicely illustrated in europium iridium hydrides. In M_2IrH_5 (M = Ca, Sr, Eu) and in mixed crystal systems with M = $Eu_{1-x}Ca_x$, $Eu_{1-x}Sr_x$, temperature-driven phase transitions occur. At room temperature, 18-electron complexes $[IrH_5]^{4-}$ are rotationally disordered with 5/6 occupancy for hydrogen atoms in a K_2PtCl_6-type arrangement. Cooling results in a cubic-to-tetragonal phase transition with partial ordering of IrH_5 pyramids that now point either upward or downward.[44] This highlights the two main factors governing solid-state structures of complex hydrides, that is, the 18-electron rule, limiting the hydrogen content, and the high mobility of hydrogen as a ligand, giving rise to disorder. For a more detailed description of crystal structures and order-disorder phase transitions of ternary hydrides of the late transition metals and their structural relationships see a recent review.[32a]

5. Solid-State Structures of Samarium Hydrides

The problem of neutron absorption gets even worse when moving from europium to samarium compounds. One has to shorten the wavelength even further in order to reduce the absorption cross section of a natural isotope mixture of samarium to reasonable values. This means doing experiments with hot neutrons at wavelengths as short as 50 pm on diffractometers with very moderate resolution (Figure 3). Our own studies have been restricted in this case to SmD_3 as a test case for the neutron diffraction method and $SmMg_2D_7$ as a member of hydrogen-rich Laves phases.

From neutron diffraction data, SmD_3 could be shown to belong to the fully ordered trigonal LaF_3 type,[45] in contrast to models with split positions, which had to be used in the formerly proposed HoD_3 type also found in NdD_3.[46] Deuterium fills tetrahedral and trigonal-planar voids in a hexagonal closest packing of samarium atoms. This structural investigation proved the feasibility of detailed structural studies by neutron diffraction on natural isotope mixtures of samarium and provided the first Sm–D distances, which are 235 pm in average in SmD_3 (Figure 11).[45]

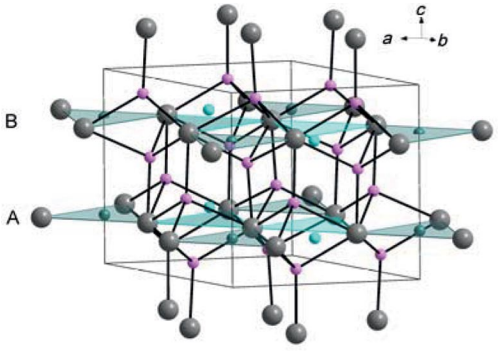

Figure 11. The crystal structure of SmD_3 in the trigonal LaF_3 type structure (Sm as large gray spheres, D1 small pink spheres in nearly tetrahedral coordination, D2 small turquoise spheres in nearly triangular coordination, D3 small dark green spheres in trigonal planar coordination; figure adapted from ref.[45]).

The hydrogenation of the cubic Laves phase $SmMg_2$ combines features of the two aforementioned Laves phase hydrides. The product, an olive-green semiconducting air-sensitive hydride of the composition $SmMg_2H_7$, has, like $EuMg_2H_6$, a very high hydrogen content, but in contrast to the latter, and like $EuPd_2$, retains the topology of the metal

atom substructure (Figure 12). Neutron diffraction showed that $SmMg_2D_7$ crystallizes in a $LaMg_2D_7$-type structure[47] with a tetragonally distorted Laves phase type metal atom structure in which deuterium fully occupies the tetrahedral and trigonal-planar interstices.[45] Thus, $SmMg_2H_7$ can be described as a tetragonally distorted, deuterium-filled Laves phase. The structural relationship between the intermetallic compound and its hydride is surprising in view of the accompanying metal-to-semiconductor transition. In situ neutron diffraction studies[48] are under way to clarify the reaction pathway of the hydrogenation.

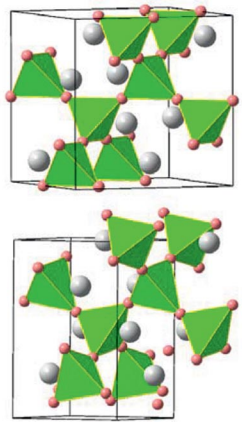

Figure 12. The crystal structures of $SmMg_2$ (cubic Laves phase, $MgCu_2$ type, top) and of the metal atom substructure of $SmMg_2D_7$ (tetragonal $LaMg_2D_7$ type, bottom). Sm atoms are shown as large gray spheres, and Mg atoms are shown as small red spheres forming Mg_4 tetrahedra.

In contrast to most other Laves phase hydrides, however, $SmMg_2H_7$ exhibits semiconducting properties and fully ordered hydrogen (deuterium) substructure. It may therefore be described by the limiting ionic formula $Sm^{3+}(Mg^{2+})_2(H^-)_7$. The magnetic ordering with both antiferromagnetic and weak ferromagnetic contributions found in $SmMg_2$ is suppressed in the hydride, probably because of the lack of conduction electrons necessary for an RKKY-like coupling of magnetic moments.[45]

Even though Laves phase hydrides are known for their application in hydrogen storage and $LnMg_2H_7$ (Ln = La, Ce, Sm) has an unusually high hydrogen content, its relatively high thermal stability hampers practical use. The latter, however, might be in reach, if these systems could be modified, for example by chemical substitution, such that the thermodynamic stability of the hydrides is lowered and at the same time the kinetics and reversibility of hydrogenation-dehydrogenation cycles improved. This might be a promising direction in the search for hydrogen storage materials.

6. Further Selected Europium and Samarium Hydrides

While in the previous sections, only those europium and samarium hydrides for which hydrogen (deuterium) positions have been determined experimentally were described in detail, some further selected compounds without complete crystal structures shall be briefly mentioned here.

Another example for the hydride fluoride analogy in ionic compounds is the class of the europium hydride halides EuHX (X = Cl, Br, I), for which the PbFCl-type structure with hydrogen in a tetrahedral void was proposed.[49] Europium may replace alkaline earth metals in complex hydrides also to form compounds such as Eu_2FeH_6, Eu_2RuH_6, Eu_2RhH_5, $EuMgNiH_4$, and $EuMg_2FeH_8$, which are presumably isostructural to their alkaline earth analogues.[50] Interstitial hydrides with europium are $EuNi_5H_{5.5}$, with a filled $CaCu_5$ type, and $EuRh_2H_{5.5}$, with a filled cubic Laves phase structure.[51] Some A_5M_3 intermetallics (A = Ca, Sr, Ba, Sm, Eu, Yb, M = Si, Ge, Sn, Pb, As, Sb, Bi) cannot be synthesized in pure form, but only stabilized by interstitial atoms like hydrogen or fluorine with formulae $A_5M_3H_{\leq 1}$.[52]

Samarium is known to form not only the trihydride as described before, but also a cubic dihydride (presumably CaF_2 type) and Sm_3H_7, for which a tetragonal Sm_3F_7 type was proposed.[53] Above 2 GPa, a cubic modification of SmH_3 was found,[54] which might be isostructural to the homologous La, Ce, and Pr compounds with a BiF_3-like structure, in which the octahedrally surrounded deuterium atoms are displaced along the space diagonal. A wealth of samarium intermetallic compounds with interstitial hydrogen are reported in the literature. Many of them have been investigated because of the application of the hydrogen-free materials as permanent magnets, such as $SmCo_5(H_{2.5})$, $Sm_2Co_{17}(H_5)$, $Sm_2Fe_{14}B(H_5)$; however, hydrogen positions have not been determined for any of them.[55] Hydrogen is used on one hand to alter the magnetic properties of the intermetallics and on the other hand as a reagent in the HDDR process (hydrogenation-decomposition-desorption-recombination), in which intermediate hydrides are formed. The latter is used for optimizing the magnetic properties of materials by controlling their microstructure.

7. Properties of Europium and Samarium Hydrides

In the above crystal chemical discussions on europium and samarium hydrides, physical properties have only been mentioned occasionally, when they were important in view of structure–property relationships and the chemical bonding situation. This last paragraph is intended to give an overview of some interesting physical properties as well as electronic structure calculations. Again, the discussion is focused on those compounds for which full crystal structure information is available. The data, some of which are summarized in Table 1, vary considerably between different sources in the literature. This seems to be the result of problems with sample purity in some cases, which are due to the strong air sensitivity of most europium and samarium hydrides.

Table 1. Selected structural and physical properties of europium and samarium hydrides.

Compound	Structure type[a]	Color	T_C /K	d_{min}(Eu–Eu) at 298 K /pm	Ref.
EuH_2	$PbCl_2$	violet	18	369	[14,15]
$EuLiH_3$	$SrTiO_3$	red	38	380	[14,25]
Eu_2MgH_6	K_2GeF_6	brown	32	372	[30]
$EuMgH_4$	$BaZnF_4$	brown	19[a]	393	[29]
$Eu_6Mg_7H_{26}$	$Ba_6Zn_7F_{26}$	red-brown		386	[30]
$Eu_2Mg_3H_{10}$	$Ba_2Ni_3F_{10}$	orange		385	[30]
$EuMg_2H_6$	$EuMg_2D_6$	red	27[a]	377[a]	[29]
$Eu_{0.6}Sr_{0.4}Mg_2H_6$	$EuMg_2D_6$	light red	15	379	[33]
Eu_2PdH_4	β-K_2SO_4	dark violet	15[a]	357[a]	[38]
$EuPdH_3$	$SrTiO_3$	black	21	384	[38,41]
Eu_2IrH_5	K_2PtCl_6	black	20	379	[44,58]
Eu_2IrH_5 (7 K)[b]	Sr_2IrD_5 (4 K)			373	
$Eu_{0.5}Ca_{1.5}IrH_5$	K_2PtCl_6	black		367	[44]
$Eu_{0.5}Ca_{1.5}IrH_5$ (10 K)[b]	Sr_2IrD_5 (4 K)			360	
$EuSrIrH_5$	K_2PtCl_6	black	<7	380	[44,58]
$EuSrIrH_5$ (7 K)[b]	Sr_2IrD_5 (4 K)			374	
SmH_3	LaF_3	brown	–	–	[45]
$SmMg_2H_7$	$LaMg_2D_7$	olive-green	–	–	[45]

[a] Results on corresponding deuterides. [b] Distances calculated from X-ray diffraction data at temperatures given, full crystal structures determined at 100 K and 120 K, respectively.

7.1. Optical and Electrical Properties

Most of the europium and samarium hydrides assumed to be ionic or complex hydrides for crystal chemical reasons given above, are colored (Table 1). This indicates semiconducting behavior in accordance with structural properties. Optical absorption measurements are rare. In EuH_2 the optical band gap was shown to be 1.85 eV,[15b] confirming its semiconducting behavior. In other cases, temperature-dependent electrical resistivity measurements allowed $EuLiH_3$, Eu_2RuH_6, and Eu_2IrH_5 to be classified as semiconductors with band gaps of 1.5, 0.08, and 0.15 eV, respectively.[25c,50b,56]

Quantum mechanical calculations were also performed in order to characterize the electronic structure and to predict physical properties of europium and samarium hydrides. The treatment of the largely localized 4f electrons, however, causes some intrinsic problems, leading sometimes to differences between theory and experiment. The band gap of 0.29 eV calculated for EuH_2[39] seems to be underestimated with respect to experimental results (see above). $EuPdH_3$ is predicted to be metallic and Eu_2PdH_4 to be a semiconductor with 0.23 eV,[39] in agreement with crystal chemical considerations.[38]

7.2. Magnetic Properties

Studying the magnetic behavior allows the distinction between Eu^{II} and Eu^{III} in the solid state. While the free ion value to be expected for the former is 7.95 μ_B for the effective magnetic moment, that of the latter is 0. All europium hydrides studied so far show ferromagnetism with Curie temperatures in the range $7\,K \leq T_C \leq 38\,K$ and effective magnetic moments of $7.3\,\mu_B \leq \mu_{eff} \leq 8.4\,\mu_B$ (Table 1). This indicates europium to be divalent in all these hydrides, in accordance with crystal structures (see section 4). Trivalent europium could not be established in a hydride matrix so far, probably due to the medium oxidizing power of hydrogen.

An interesting question is on the magnetic coupling of the europium ions in the ferromagnetic state. Since most investigated compounds are not metallic, europium hydrides are semiconducting ferromagnets at low temperatures and an RKKY mechanism with coupling through conduction electrons is ruled out. While Eu–Eu distances are too long for a direct 4f–4f overlap (Table 1), another type of exchange has been proposed. Similar to the situation in europium chalcogenides,[57] a 4f electron may be transferred to an empty conduction 5d state. The 5d orbitals of neighboring europium ions may overlap, thus establishing a ferromagnetic coupling, for example in EuH_2.[15] Similar coupling of magnetic moments of europium after intra-atomic 4f–5d transfer is assumed to cause ferromagnetism in Eu_2IrH_5.[58] In $EuLiH_3$ Ueno's model of a respective 4f–6s transfer mechanism[59] has been considered more appropriate.[60] Such direct coupling after 4f–5d or 4f–6s transfer mechanisms should depend strongly on Eu–Eu distances. Neither the minimum Eu–Eu distances (Table 1) nor average distances, however, show a clear correlation to ferromagnetic ordering temperatures, such that other exchange mechanism may also be present, complicating the picture considerably.

Curie temperatures are somewhat higher for ionic hydrides than for most complex europium hydrides in which hydrogen is bonded covalently within a complex hydrido transition metal complex (Table 1). This observation may point to a possible involvement of hydrogen atoms in the coupling of magnetic moments. Whether or not they participate in exchange mechanisms is not clear as yet. The difference between the ferromagnetic $EuLiH_3$ and the isostructural antiferromagnetic $EuTiO_3$ was explained by the inability of $1s^2$-configured H^- to participate in superexchange like O^{2-}, that is, no antiferromagnetic coupling of nearest neighbors is considered to be possible in that case.[25] On the other hand, other authors have proposed superexchange through hydride anions, for example in EuH_2 or in oxide hydrides.[61]

In such discussions, it has to be considered that ferromagnetic transition temperatures reported in the literature may vary considerably for some compounds, pointing at possible problems with sample purity, which is not surprising in view of the strong air sensitivity of the hydrides, resulting in decomposition and oxidation to Eu^{III}.

SmH_3 and $SmMg_2H_7$ are paramagnetic down to the lowest measured temperatures of 2 K with effective magnetic moments of 0.63 and 0.57 μ_B, respectively.[45] Apparently, the above-mentioned possible coupling mechanisms are not strong enough for cooperative magnetic phenomena in hydrides with Sm^{III}, which exhibits a theoretical free ion value for the magnetic moment of only 0.845 μ_B.

8. Conclusions

Europium and samarium hydrides show a very rich crystal chemistry, ranging from typical ionic hydrides following the hydride-fluoride analogy to complex transition metal hydrides and interstitial hydrides. Crystal structure, electrical, and magnetic properties prove europium to be divalent in hydrides investigated so far. Samarium, on the other hand, is easily transformed to a trivalent oxidation state in its hydrides and shows similarities to hydrides of other trivalent lanthanides. The crystal structures could only be solved and refined by a combination of X-ray (synchrotron) and neutron diffraction methods. The problem of neutron absorption of europium and samarium, hampering the solution of crystal structures and limiting the available structural information, may be overcome either by the use of isotopically pure material or by careful choice of the neutron wavelength and the sample geometry on high-flux neutron diffractometers. The latter aspect underlines the importance of instrumental developments on synchrotron and neutron sources.

[1] a) R. B. King, *Coord. Chem. Rev.* **2000**, *200–202*, 813–829; b) S. Aldridge, A. J. Downs, *Chem. Rev.* **2001**, *101*, 3305–3365; c) H. Kohlmann, "Metal Hydrides" in *Encyclopedia of Physical Sciences and Technology* (Ed.: R. A. Meyers), 3rd ed., Academic Press, San Diego, **2002**, vol. 9, pp. 441–458; d) K. Yvon, "Metal Hydrides: Transition Metal Hydride Complexes" in *Encyclopedia of Materials: Science and Technology* (Eds.: K. H. J. Buschow, R. W. Cahn, M. C. Flemings, B. Ilschner, E. J. Kramer, S. Mahajan), Elsevier, Amsterdam, **2004**, pp. 1–9.

[2] a) A. Züttel, *Naturwissenschaften* **2004**, *91*, 157–172; b) J. Graetz, *Chem. Soc. Rev.* **2009**, *38*, 73–82.

[3] a) K. Yvon, "Locating Hydrogen in Metal Hydrides by X-ray and Neutron Diffraction" in *Neutron Scattering from Hydrogen in Materials* (Ed.: A. Furrer), World Scientific, Singapore, **1994**, pp. 84–96; b) W. Bronger, "Synthesis and Structure of New Metal Hydrides" in *Neutron Scattering from Hydrogen in Materials* (Ed.: A. Furrer), World Scientific, Singapore, **1994**, pp. 97–109; c) G. Auffermann, P. Müller, W. Bronger, *Z. Anorg. Allg. Chem.* **2004**, *630*, 2113–2124.

[4] a) V. P. Ting, P. F. Henry, C. C. Wilson, H. Kohlmann, M. T. Weller, *Phys. Chem. Chem. Phys.* **2010**, *12*, 2083–2088; b) M. T. Weller, P. F. Henry, V. P. Ting, C. C. Wilson, *Chem. Commun.* **2009**, 2973–2989.

[5] J. Rodriguez-Carvajal, FullProf.2k, Version 3.70 - Jul2006-ILL JRC, **2006**, unpublished.

[6] A. C. Larson, R. B. Von Dreele, *General Structure Analysis System* (GSAS), Los Alamos National Laboratory Report LAUR 86–748, **2000**.

[7] V. F. Sears, *Thermal-Neutron Scattering Lengths and Cross Sections for Condensed-Matter Research*, Chalk River Nuclear Laboratories, Chalk River, Ontario, AECL-8490, **1984**.

[8] V. F. Sears, *Neutron News* **1992**, *3*, 26–37.

[9] M. Haïssinsky, J.-P. Adloff, *Radiochemical Survey of the Elements*, Elsevier, Amsterdam, **1965**.

[10] J. E. Lynn, *J. Appl. Crystallogr.* **1989**, *22*, 476–482.

[11] T. C. Hansen, P. F. Henry, H. E. Fischer, J. Torresgrossa, P. Convert, *Meas. Sci. Technol.* **2008**, *19*, 034001.

[12] H. E. Fischer, G. J. Cuello, P. Palleau, D. Feltin, A. C. Barnes, Y. S. Badyal, J. M. Simonson, *Appl. Phys. A: Mater. Sci. Process* **2002**, *74*, [Suppl.], S160–S162.

[13] D. Schmitt, B. Ouladdiaf, *J. Appl. Crystallogr.* **1998**, *31*, 620–624.

[14] H. Kohlmann, K. Yvon, *J. Alloys Compd.* **2000**, *299*, L16–L20.

[15] a) R. L. Zanowick, W. E. Wallace, *Phys. Rev.* **1962**, *126*, 537–539; b) R. Bischof, E. Kaldis, P. Wachter, *J. Magn. Magn. Mater.* **1983**, *31–34*, 255–256; c) R. Bischof, E. Kaldis, P. Wachter, *J. Solid State Chem.* **1985**, *111*, 139–144.

[16] a) R. E. Bischof, E. Kaldis, *Helv. Phys. Acta* **1982**, *55*, 348–350; b) K. I. Hardcastle, J. C. Warf, *Inorg. Chem.* **1966**, *5*, 1728–1735.

[17] W. L. Korst, J. C. Warf, *Acta Crystallogr.* **1956**, *9*, 452–454.

[18] A. F. Andresen, A. J. Maeland, D. Slotfeldt-Ellingsen, *J. Solid State Chem.* **1977**, *20*, 93–101.

[19] N. E. Brese, M. O'Keefe, R. B. von Dreele, *J. Solid State Chem.* **1990**, *88*, 571–576.

[20] W. Bronger, C. S. Chi, P. Müller, *Z. Anorg. Allg. Chem.* **1987**, *545*, 69–74.

[21] P. Fischer, J. Schefer, K. Tichy, R. Bischof, E. Kaldis, *J. Less-Common Met.* **1983**, *94*, 151–155.

[22] W. Bronger, *Z. Anorg. Allg. Chem.* **1996**, *622*, 9–16.

[23] W. Jeitschko, *Acta Crystallogr., Sect. B: Struct. Crystallogr. Cryst. Chem.* **1968**, *24*, 930–934.

[24] C. E. Messer, K. Hardcastle, *Inorg. Chem.* **1964**, *3*, 1327–1328.

[25] a) J. E. Greedan, *J. Phys. Chem. Solids* **1971**, *32*, 1039–1046; b) C.-L. Chien, J. E. Greedan, *Phys. Lett. A* **1971**, *36*, 197–198; c) J. E. Greedan, *J. Phys. Chem. Solids* **1971**, *32*, 1039–1046.

[26] K. Yvon, H. Kohlmann, B. Bertheville, *Chimia* **2001**, *55*, 505–509.

[27] F. Gingl, K. Yvon, P. Fischer, *J. Alloys Compd.* **1992**, *187*, 105–111.

[28] F. Gingl, K. Yvon, P. Fischer, *J. Alloys Compd.* **1994**, *206*, 73–75.

[29] H. Kohlmann, F. Gingl, T. Hansen, K. Yvon, *Angew. Chem.* **1999**, *111*, 2145–2147; *Angew. Chem. Int. Ed.* **1999**, *38*, 2029–2032.

[30] H. Kohlmann, B. Bertheville, T. Hansen, K. Yvon, *J. Alloys Compd.* **2001**, *322*, 59–68.

[31] K. Yvon, B. Bertheville, *J. Alloys Compd.* **2006**, *425*, 101–108.

[32] a) H. Kohlmann, *Z. Kristallogr.* **2009**, *224*, 454–460; b) H. Kohlmann, *Z. Kristallogr.* **2010**, *225*, 195–200.

[33] H. Kohlmann, K. Yvon, Y. Wang, *J. Alloys Compd.* **2005**, *393*, 11–15.

[34] a) A. Möller, *Z. Anorg. Allg. Chem.* **2001**, *627*, 2625–2629; b) A. Möller, *Z. Anorg. Allg. Chem.* **2005**, *631*, 2285–2296.

[35] F. Gingl, A. Hewat, K. Yvon, *J. Alloys Compd.* **1997**, *253–254*, 17–20.

[36] B. Bertheville, H. Kohlmann, D. Sheptyakov, K. Yvon, *J. Alloys Compd.* **2003**, *356–357*, 128–132.

[37] F. Gingl, K. Yvon, T. Vogt, *J. Alloys Compd.* **1997**, *256*, 155–158.

[38] H. Kohlmann, H. E. Fischer, K. Yvon, *Inorg. Chem.* **2001**, *40*, 2608–2613.

[39] E. Orgaz, *J. Alloys Compd.* **2003**, *356–357*, 191–194.

[40] A. V. Irodova, V. A. Somenkov, S. Sh. Shil'stein, L. N. Padurets, *Sov. Phys. Crystallogr.* **1978**, *23*, 591–592.

[41] a) K. H. J. Buschow, R. L. Cohen, K. W. West, *J. Appl. Phys.* **1977**, *48*, 5289–5295; b) E. Orgaz, V. Mazel, M. Gupta, *Phys. Rev. B: Condens. Matter Mater. Phys.* **1996**, *54*, 16124–16130.

[42] a) H. Kohlmann, G. Renaudin, K. Yvon, C. Wannek, B. Harbrecht, *J. Solid State Chem.* **2005**, *178*, 1292–1300; b) H. Kohlmann, F. Müller, K. Stöwe, A. Zalga, H. P. Beck, *Z. Anorg. Allg. Chem.* **2009**, *635*, 1407–1411.

[43] a) V. A. Somenkov, A. V. Irodova, *J. Less-Common Met.* **1984**, *101*, 481–492; b) H. Kohlmann, K. Yvon, *J. Alloys Compd.* **2000**, *309*, 123–126; c) H. Kohlmann, F. Fauth, P. Fischer, A. V. Skripov, K. Yvon, *J. Alloys Compd.* **2001**, *327*, L4–L9.

[44] H. Kohlmann, R. O. Moyer Jr., T. Hansen, K. Yvon, *J. Solid State Chem.* **2003**, *174*, 35–43.

[45] H. Kohlmann, F. Werner, K. Yvon, G. Hilscher, M. Reissner, G. J. Cuello, *Chem. Eur. J.* **2007**, *13*, 4178–4186.

[46] G. Renaudin, P. Fischer, K. Yvon, *J. Alloys Compd.* **2000**, *313*, L10–L14.

[47] F. Gingl, K. Yvon, T. Vogt, A. Hewat, *J. Alloys Compd.* **1997**, *253–254*, 313–317.
[48] H. Kohlmann, N. Kurtzemann, R. Weihrich, T. Hansen, *Z. Anorg. Allg. Chem.* **2009**, *635*, 2399–2405.
[49] H. P. Beck, A. Limmer, *Z. Naturforsch., Teil B* **1982**, *37*, 574–578.
[50] a) B. Huang, F. Bonhomme, P. Selvam, K. Yvon, P. Fischer, *J. Less-Common Met.* **1991**, *171*, 301–311; b) J. S. Thompson, R. O. Moyer Jr., R. Lindsay, *Inorg. Chem.* **1975**, *14*, 1866–1869; c) R. O. Moyer Jr., B. J. Burnim, R. Lindsay, *J. Solid State Chem.* **1996**, *121*, 56–60; d) B. Huang, K. Yvon, P. Fischer, *J. Alloys Compd.* **1994**, *204*, L5–L8; e) B. Huang, K. Yvon, P. Fischer, *J. Alloys Compd.* **1995**, *227*, 121–124.
[51] a) Z. Gavra, J. J. Murray, L. D. Calvert, J. B. Taylor, *J. Less-Common Met.* **1985**, *105*, 291–301; b) K. H. J. Buschow, R. L. Cohen, K. W. West, *J. Appl. Phys.* **1977**, *48*, 5289–5295.
[52] a) E. A. Leon-Escamilla, P. Dervenagas, C. Stassis, J. D. Corbett, *J. Solid State Chem.* **2010**, *183*, 114–119; b) E. A. Leon-Escamilla, J. D. Corbett, *Chem. Mater.* **2006**, *18*, 4782–4792; c) E. A. Leon-Escamilla, J. D. Corbett, *J. Solid State Chem.* **2001**, *159*, 149–162; d) E. A. Leon-Escamilla, J. D. Corbett, *Inorg. Chem.* **2001**, *40*, 1226–1233.
[53] O. Greis, P. Knappe, H. Müller, *J. Solid State Chem.* **1981**, *39*, 49–55.
[54] T. Palasyuk, M. Tkacz, *Solid State Commun.* **2007**, *141*, 302–305.
[55] a) H. Zijlstra, F. F. Westendorp, *Solid State Commun.* **1969**, *7*, 857–859; b) J. Evans, C. E. King, I. R. Harris, *J. Mater. Sci.* **1985**, *20*, 817–820; c) P. l'Héritier, P. Chaudouët, R. Madar, A. Rouault, J.-P. Sénateur, R. Fruchart, *C R. Acad. Sci., Ser. II: Mec., Phys., Chim., Sci. Terre Univers.* **1984**, *299*, 849–852.
[56] R. O. Moyer Jr., R. Lindsay, *J. Less-Common Met.* **1980**, *70*, P57–P67.
[57] T. Kasuya, A. Yanase, *Rev. Mod. Phys.* **1968**, *40*, 684–696.
[58] a) Z. M. Stadnik, R. O. Moyer Jr., *J. Less-Common Met.* **1984**, *98*, 159–164; b) R. Lindsay, R. O. Moyer Jr., W. Strange, B. J. Burnim, *J. Alloys Compd.* **1996**, *243*, 90–94.
[59] K. Ueno, A. Yanase, T. Kasuya, *J. Magn. Magn. Mater.* **1983**, *31–34*, 427–428.
[60] K. Kojima, T. Imai, K. Hiraoka, T. Hihara, Y. Kasamatsu, *J. Phys. Soc. Jpn.* **1987**, *56*, 4141–4149.
[61] a) A. Mustachi, *J. Phys. Chem. Solids* **1974**, *35*, 1447–1450; b) S. J. Blundell, I. M. Marshall, F. L. Pratt, M. A. Hayward, E. J. Cussen, J. B. Claridge, M. Bieringer, C. J. Kiely, M. J. Rosseinsky, *Phys. B (Amsterdam)* **2003**, *326*, 527–531.

Received: January 31, 2010
Published Online: May 25, 2010

